ELSEVIER

Journal of Nuclear Materials 283–287 (2000) 977–981

journal of nuclear materials

www.elsevier.nl/locate/jnucmat

Fracture behavior of high-strength, high-conductivity copper alloys

M. Li [a], J.K. Heuer [a], J.F. Stubbins [a,*], D.J. Edwards [b]

[a] *Department of Nuclear, Plasma and Radiological Engineering, 214 Nuclear Engineering Laboratory, University of Illinois, 103 South Goodwin Avenue, Urbana, IL 61801-2984, USA*

[b] *Pacific Northwest National Laboratory, P.O. Box 999, Richland, WA 99352, USA*

Abstract

The fracture behavior of three copper alloys, namely, one dispersion-strengthened alloy: GlidCop™CuAl25, and two precipitation-hardened alloys: Hycon3HP™CuNiBe and Elbrodur CuCrZr, was investigated in the temperature range 20–300°C in vacuum. The results show that all these three alloys experienced a loss of fracture resistance with increasing test temperature. In the case of the CuNiBe alloy, the fracture resistance drops very rapidly as test temperature increases, and the other two alloys also experience drops in toughness, but not quite to the same extent. In fact, the fracture resistance of CuCrZr is affected only moderately by test temperature. The reduction of fracture resistance with increasing temperature in vacuum shows that the environment is not the only factor responsible for poor toughness. Further, microstructural analysis of the CuNiBe alloy shows that changes in grain boundary microstructure resulted from discontinuous precipitation. This is assumed to have a significant effect on the fracture behavior of this alloy.

1. Introduction

High-strength copper alloys with high thermal conductivity have been considered as candidate materials for the first wall and the divertor heat sink applications in the International Thermonuclear Experimental Reactor (ITER) design. While the copper alloys exhibit superior strength compared to unalloyed copper, they all experience a loss of fracture toughness with increasing temperature [1–3]. Their low fracture toughness is their major restriction for applications, particularly at elevated temperatures. The fracture toughness degradation with increasing temperature has been suggested to be related to environmental and/or impurity effects [2]. The purpose of this study is to investigate the fracture behavior of three copper alloys at elevated temperature in vacuum, and to elucidate the mechanisms controlling fracture behavior.

2. Experimental procedure

Three copper alloys, namely, GlidCop™CuAl25 (0.25 wt% Al), Hycon3HP™CuNiBe (1.92 wt% Ni, 0.35 wt% Be), and Elbrodur CuCrZr (0.65 wt% Cr, 0.1 wt% Zr) were studied. The GlidCop™CuAl25 alloy (Heat #C-8064, ITER grade 0) was cross-rolled, annealed, and boron deoxidized. Hycon3HP™CuNiBe alloy (Heat #46546) was in the HT tempered condition (cold worked and aged), and then heat-treated again to produce an AT tempered condition (solutionized, quenched, and aged). Elbrodur CuCrZr alloy (Heat #AN4946) was in the cold worked and aged condition (F37 temper).

Specimens with two types of geometry were tested: one type was a subsize notched-tensile specimen with a 3.0 mm gauge diameter, oriented in the L–S directions. The notches at the center of gauge section were perpendicular to the rolling direction. The second type was a subsize four-point bend bar specimen of $47.2 \times 6.6 \times 3.0\ \text{mm}^3$, oriented in the L–S directions with the notches perpendicular to the rolling direction. The tensile and fracture tests were performed in the temperature range 20–300°C in vacuum on an Instron

* Corresponding author. Tel.: +1-217 333 2295; fax: +1-217 333 2906.

E-mail address: jstubbin@uiuc.edu (J.F. Stubbins).

0022-3115/00/$ - see front matter
PII: S0022-3115(00)00316-0

closed-loop servohydraulic test frame equipped with a vacuum furnace system. Extensometry was achieved with a capacitive displacement device. An MTS 5.08-mm gauge span extensometer was used to calibrate the Capacitec capacitance probe at room temperature for each alloy. A cross-head speed of 0.006 mm/s was selected for mechanical testing. This corresponds to a strain rate of the order of 10^{-4} s^{-1}. Considering the strain rate sensitivity of copper alloys [4], the same strain rate was chosen for each alloy. The fatigue precracking was performed on the four-point bend bar specimens at room temperature in air. A cross-head speed of 0.013 mm/s was selected in the four-point bending tests to satisfy ASTM standard E399. The heating rate at elevated temperature tests was approximately 0.058°C/s. After reaching the desired temperature, the specimens were held in vacuum at temperature approximately for one half hour to stabilize the temperature before loading. All tests were controlled with specialized LABVIEW software.

The failed specimens were first examined using optical microscopy. Typical fracture surfaces were examined with a Hitachi S-800 scanning electron microscopy operated at 10 kV. A Perkin Elmer Phi 660 Auger microprobe was used to examine the fracture surface chemistry of the notched tensile specimens.

3. Results and discussion

3.1. Fracture behavior of three copper alloys

Tensile results of three copper alloys tested at the temperature of 20°C, 200°C and 300°C in vacuum are shown in Fig. 1. It is noted that the plastic deformation and fracture behavior were found to be quite different among the three copper alloys at elevated testing temperature. GlidCop™CuAl25 shows significant plastic deformation at all the three test temperatures. The fracture load and displacement decreased as the temperature increased. Elbrodur CuCrZr alloy shows larger plastic deformation than GlidCop™CuAl25 alloy, and the strength and ductility do not change significantly with increasing temperature. In contrast, Hycon3HP™CuNiBe alloy shows brittle behavior at all three test temperatures and much higher strength than the other two alloys. Brittle fracture in the CuNiBe alloy is more evident with increasing test temperature, and the apparent fracture strength decreases considerably.

Fracture energy for each of the three copper alloys was obtained by integrating the area under the load–displacement curves. Fig. 2 shows the fracture energy as a function of temperature for all the three copper alloys. The fracture energies of GlidCop™CuAl25 and Hycon3HP™CuNiBe decrease rapidly as the test temperature increases. For Elbrodur CuCrZr alloy, the fracture

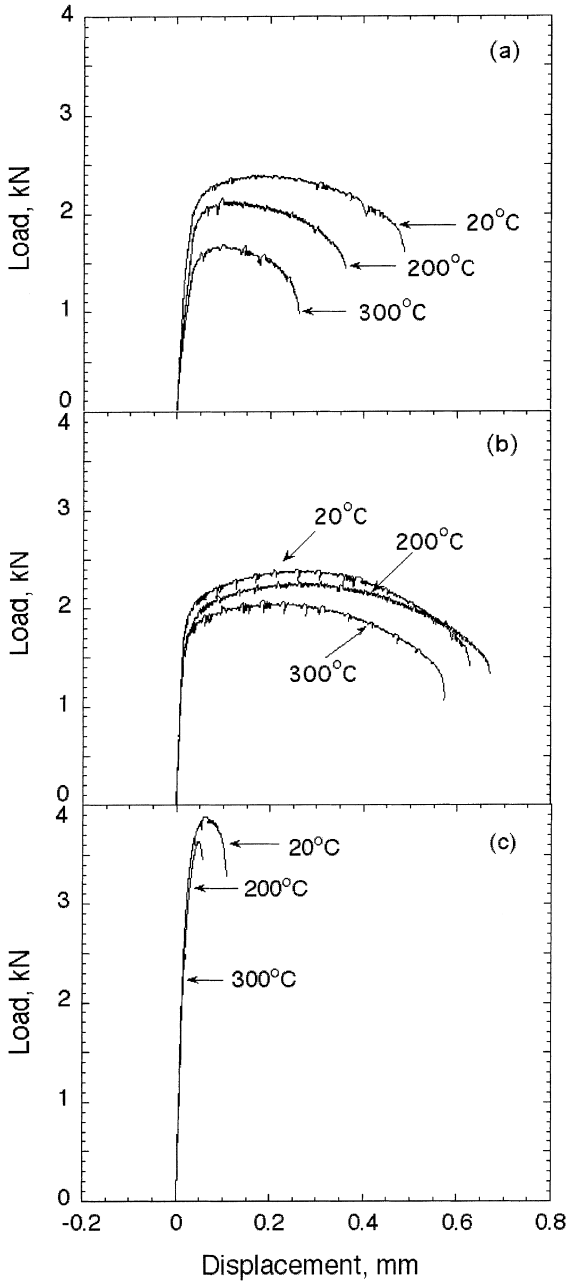

Fig. 1. Tensile load–displacement curves of: (a) CuAl25; (b) CuCrZr; (c) CuNiBe at different temperatures in vacuum.

energy does not show significant change at 200°C, but decreases at 300°C. Comparing these three alloys, the fracture energy of the CuCrZr alloy is highest, and the fracture energy of the CuNiBe alloy is lowest at all temperatures. It should be pointed out that all three copper alloys show a trend of decreasing fracture resistance with increasing temperature even when tested in

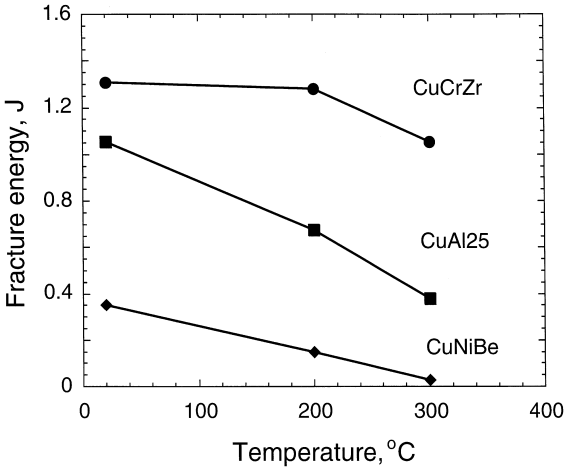

Fig. 2. Fracture resistance vs temperature of the three copper alloys tested in tension in vacuum.

vacuum. This indicates that the poor fracture toughness is not totally due to an environmental effect.

The fracture toughness, K_Q, of the CuNiBe alloy was measured following ASTM E399 over the temperature range 20–300°C in vacuum in four-point bending tests, and the results are shown in Fig. 3. The rapid drop of fracture toughness in the CuNiBe alloy with increasing temperature further demonstrates that the environmental effect, if any, is not the only factor responsible for poor toughness of the copper alloy at elevated temperature. Some more critical factors are responsible for the poor fracture resistance. Although no valid fracture toughness values were obtained for the CuAl25 and CuCrZr alloys due to limited constraint in the bend bar specimens, the macroscopic observations of the failed specimens of all the three copper alloys by optical microscopy were quite revealing. The CuCrZr alloy showed large plastic zones around notches at both room temperature and 300°C without visible crack extension. In contrast, the CuNiBe alloy did not show a visible plastic zone around the initial crack even for room temperature loading. A rather interesting feature was observed in the CuAl25 alloy. It was found that not only a relatively large plastic zone was formed around the initial crack, but also the cracks extended in the opposite directions perpendicular to the initial cracking direction at both RT and 300°C (see Fig. 4). This feature indicates that a strong preference for crack extension is along the rolling direction rather than the initial crack direction.

3.2. Fracture surface microanalysis

The fracture surface morphologies of the notched tensile specimens for each of the three copper alloys are shown in Fig. 5. The CuAl25 alloy shows a large amount of plasticity-induced microvoid formation at room temperature and elevated temperature. The dimple size is not uniformly distributed. Similarly, the CuCrZr alloy shows microvoid coalesce cracking at both temperatures. The depth and width of the observed dimples are similar at each temperature. The dimple sizes of the CuCrZr alloy are larger compared to those of the CuAl25 alloy. At higher magnification, cracked second-phase particles are visible inside dimples. They are not found in the CuAl25 alloy specimens. The CuNiBe alloy shows a mixed mode of transgranular fracture and intergranular fracture. As the test temperature increases, the intergranular fracture becomes more evident corresponding to the decrease in fracture toughness.

The AES results taken from the fracture surfaces of each alloy after testing at various temperatures were

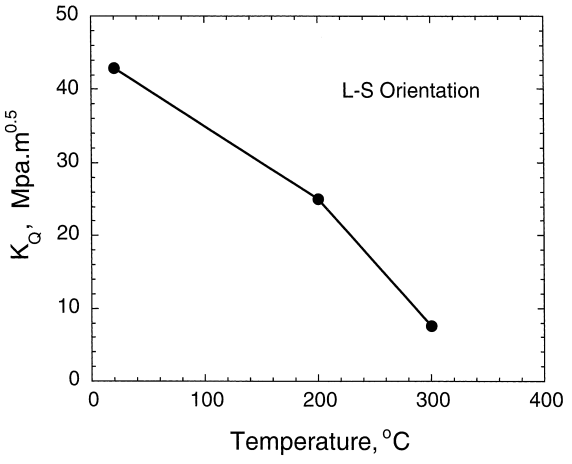

Fig. 3. Fracture toughness vs temperature of the CuNiBe alloy in bending test in vacuum.

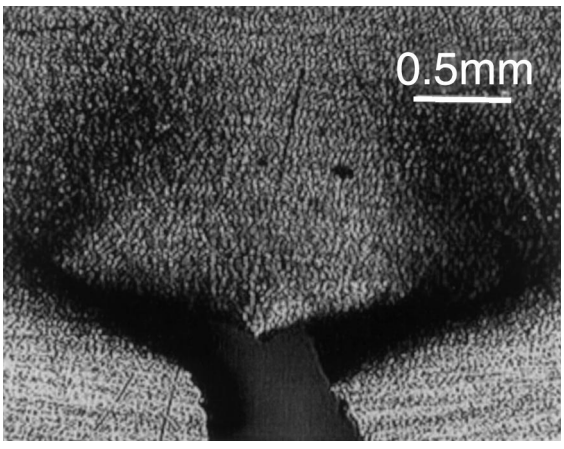

Fig. 4. Optical micrograph showing the fracture feature of bend bar specimen of the CuAl25 alloy at 300°C.

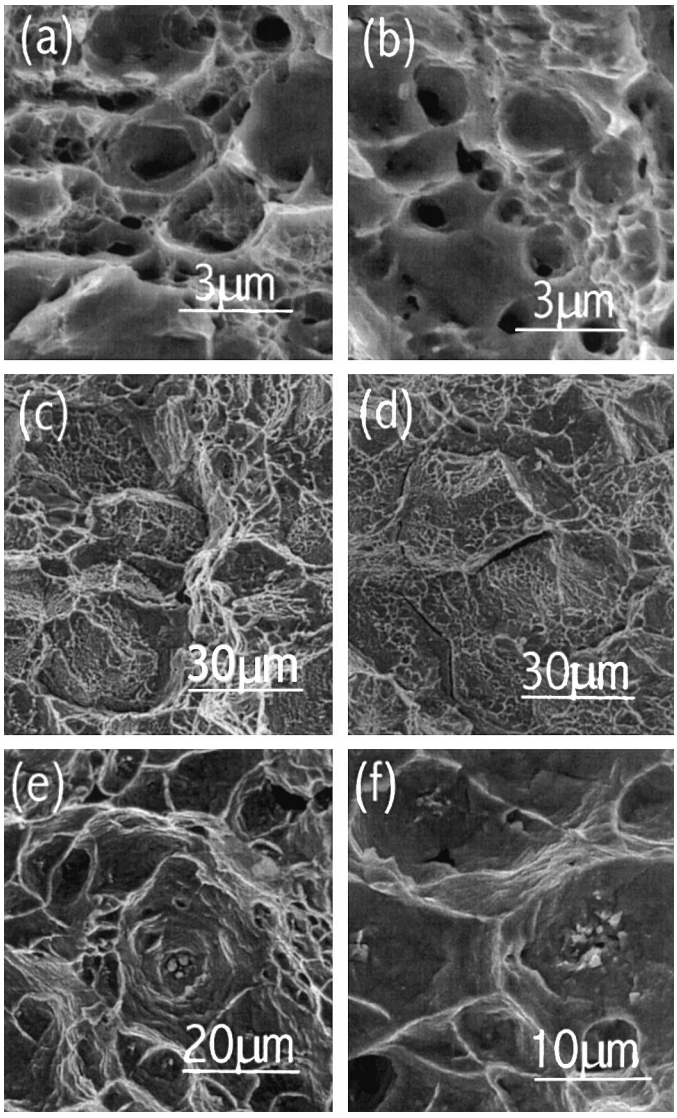

Fig. 5. Scanning electron fractographs of tensile specimens of: (a) CuAl25 at 20°C; (b) CuAl25 at 200°C; (c) CuNiBe at 20°C; (d) CuNiBe at 300°C; (e) CuCrZr at 20°C; (f) CuCrZr at 300°C.

complicated by the formation of thin oxide and contamination film at the free fracture surface. However, no changes in average surface chemistry, compared to bulk values, could be detected.

4. Conclusions

All the three copper alloys experienced a loss of fracture resistance with increasing test temperature. The fracture toughness of the CuNiBe alloy drops very rapidly as test temperature increases, and the other two alloys also experience drops in toughness, but not as much as the CuNiBe alloy.

The fracture toughness degradation with increasing temperature has been suggested to be related to environmental and/or impurity effects. However, the current results show that the environment cannot be the predominant factor responsible for poor toughness.

The fracture surface morphology reveals that both the CuCrZr alloy and the CuAl25 alloys display ductile fracture by microvoid coalesce in the temperature range 20–300°C. The CuNiBe alloy shows mixed mode of the transgranular and intergranular fracture even at room temperature. With increasing temperature, grain

boundary cracking is more predominant. Discontinuous precipitation at grain boundaries in the CuNiBe alloy is proposed to have a detrimental effect on the toughness of this alloy, especially at elevated temperature.

Acknowledgements

This work was supported by the Associated Western Universities (AWU) through a grant from the Pacific Northwest National Laboratory (PNNL) under the US DOE Fusion Materials Program, as well as by OMG Americas, and Brush Wellman. We would like to express our appreciation to D.J. Edwards, PNNL, and the US DOE Fusion Materials Program for supplying the GlidCop and Hycon materials, produced by OMG Americas, and Brush Wellman, respectively. We would also like to thank S.J. Zinkle, ORNL, for supplying the CuCrZr alloy. The Advanced Materials Testing and Evaluation Laboratory (AMTEL), UIUC and the Center for Microanalysis of Materials in Seitz Materials Research Laboratory, UIUC provided the mechanical testing facilities and microanalysis facilities.

References

[1] S.J. Zinkle, S.A. Fabritsiev, Fusion Materials Semiannual Progress Report for Period Ending 31 March 1994, DOE/ER-0313/16.
[2] D.J. Alexander, S.J. Zinkle, A.F. Rowcliffe, J. Nucl. Mater. 271&272 (1999) 429.
[3] B.N. Singh, D.J. Edwards, M. Eldrup, P. Toft, J. Nucl. Mater. 249 (1997) 1.
[4] S.J. Zinkle, W.S. Eatherly, Fusion Materials Semiannual Progress Report for Period Ending 30 June 1997, DOE/ER-0313/22.